

# SSB Facilitates Fork-Substrate Discrimination by the PriA DNA Helicase

Hui Yin Tan and Piero R. Bianco\*

Cite This: *ACS Omega* 2021, 6, 16324–16335

Read Online

ACCESS |



Metrics &amp; More

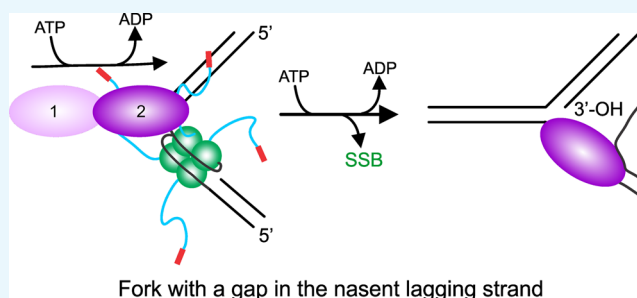


Article Recommendations



Supporting Information

**ABSTRACT:** Primosomal protein A (PriA) is a member of helicase SuperFamily 2. Its role *in vivo* is to reload the primosome onto resurrected replication forks resulting in the restart of the previously stalled DNA replication process. Single-stranded DNA-binding protein (SSB) plays a key role in mediating activities at replication forks and interacts both physically and functionally with PriA. To gain a mechanistic insight into the PriA–SSB interaction, a coupled spectrophotometric assay was utilized to characterize the ATPase activity of PriA *in vitro* in the presence of fork substrates. The results demonstrate that SSB enhances the ability of PriA to discriminate between fork substrates as much as 140-fold. This is due to a significant increase in the catalytic efficiency of the helicase induced by SSB. This interaction is species-specific as bacteriophage gene 32 protein cannot substitute for the *Escherichia coli* protein. SSB, while enhancing the activity of PriA on its preferred fork decreases both the affinity of the helicase for other forks and the catalytic efficiency. Central to the stimulation afforded by SSB is the unique ability of PriA to bind with high affinity to the 3'-OH placed at the end of the nascent leading strand at the fork. When both the 3'-OH and SSB are present, the maximum effect on the ATPase activity of the helicase is observed. This ensures that PriA will load onto the correct fork, in the right orientation, thereby ensuring that replication restart is directed to only the template lagging strand.



## INTRODUCTION

DNA replication is prone to various challenges that stall or delay the progression of forks.<sup>5</sup> Challenges include damage to the template, shortage of DNA synthesis precursors, secondary structure, and bound proteins.<sup>6–8</sup> The repair of stalled replication forks frequently requires the actions of one or more DNA helicases.<sup>9</sup> These critical enzymes harness the chemical, free energy of ATP hydrolysis to catalyze the unwinding of double-stranded DNA (dsDNA).<sup>10,11</sup> Many DNA helicases can act on unusual DNA structures such as Holliday junctions (HJs), stalled replication forks, and recombination intermediates.<sup>12–15</sup>

Primosomal protein A (PriA) is one such DNA helicase that was originally identified as an essential factor required for the conversion of the complementary strand of  $\phi$ X174 to the replicative form during the initial stage of DNA replication.<sup>16,17</sup> It is also required for bacteriophage Mu transposition and DnaA-independent replication of pBR322.<sup>18,19</sup> During the  $\phi$ X174 life cycle, PriA binds to a DNA hairpin structure known as the *n'*-primosome assembly site (PAS), leading to the subsequent assembly of the primosome, a complex responsible for primer RNA synthesis and duplex DNA unwinding at a replication fork.<sup>20,21</sup> PAS sites also occur near the origin of pBR322 and can function as origins of DNA replication.<sup>22,23</sup> In contrast, in the Mu life cycle, PriA directs the assembly of the

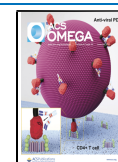
preprimosome onto Mu forks following transpososome disassembly.<sup>2,19</sup>

The 82 kDa PriA protein consists of two domains.<sup>24,25</sup> The N-terminal 181 aa is associated with DNA binding, while the C-terminal 551 aa contains the ATP binding and DNA helicase motifs which are interrupted by two, C4-type zinc finger motifs.<sup>26</sup> These Zn-finger motifs are essential for *in vitro* primosome assembly on PAS, recombination-dependent DNA replication *in vivo*, and interactions with other primosomal proteins.<sup>27–29</sup> The DNA binding properties of PriA, mediated by the N-terminus, are consistent with its activity at stalled replication forks. It binds with high affinity to D-loops and to model, fork structures *in vitro*.<sup>2,30–32</sup> This binding is mediated through specificity for DNA strands with accessible 3'-ends.<sup>30,33</sup> Specificity is provided by a 3'-terminus binding pocket located in the OB-fold in the N-terminus of the protein.<sup>34</sup>

Received: February 8, 2021

Accepted: May 19, 2021

Published: June 15, 2021



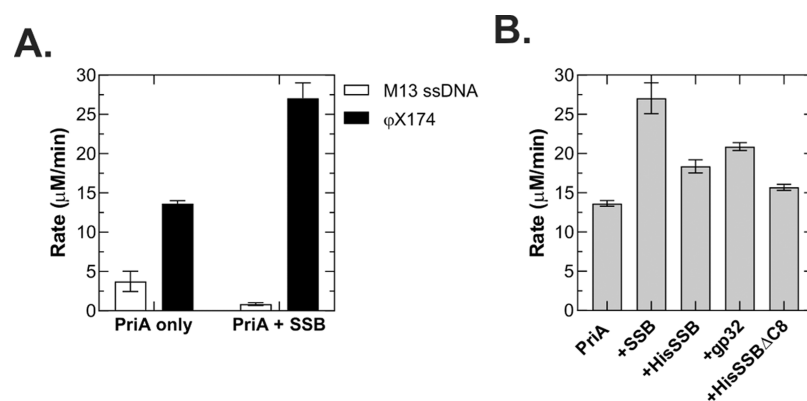


**Figure 1.** PriA exhibits ssDNA-dependent ATPase activity on  $\phi$ X174 DNA that is stimulated only by SSBs. (A) SSB enhances the ATPase activity of PriA on  $\phi$ X174 but inhibits activity in the presence of M13 ssDNA. Similar results have been published previously, but these assays were redone to permit a direct comparison to the data in B.<sup>1,2</sup> (B) SSBs increase the ATPase activity of PriA in the presence of  $\phi$ X174 ssDNA. Assays were performed as described in the [Materials and Methods](#) and contained 10  $\mu$ M nucleotides of ssDNA, 20 nM PriA, and 1  $\mu$ M SSBs (where indicated). Reactions were initiated by the addition of PriA following a 5 min incubation of all other components at 37 °C. Assays were done in duplicate on the same day.

PriA has been assigned to helicase SuperFamily 2 and has been shown to unwind DNA with a 3'  $\rightarrow$  5' polarity *in vitro*.<sup>35–37</sup> DNA unwinding is fueled by the hydrolysis of ATP (dATP), is site-specific (i.e., PAS), structure-specific, and single-stranded DNA (ssDNA)-dependent as the protein does not bind to dsDNA.<sup>30,38,39</sup> Also, DNA unwinding of model fork substrates is stimulated by the single-stranded DNA-binding protein (SSB).<sup>40</sup> This stimulation involves both a physical and a functional interaction between the two proteins.<sup>38,41–43</sup> As for several other proteins at the replication fork such as RecG, an ATP-dependent DNA helicase, the physical interaction is mediated *via* the linker domain of SSB and the OB-fold in PriA.<sup>44</sup>

Once bound to a stalled replication fork, PriA displays two types of activities. The 3'  $\rightarrow$  5' helicase activity is responsible for unwinding both the parental duplex ahead of the fork and the lagging-strand arm in an ATP-hydrolysis-dependent manner.<sup>2,35,40</sup> The ATPase activity of the enzyme is also required for substrate discrimination.<sup>45</sup> The second activity is the loading of DnaB onto the lagging-strand template *via* a complex series of protein–protein interactions reminiscent of primosome assembly for  $\phi$ X174 DNA.<sup>2,21,46,47</sup> Once DnaB has been loaded, a new replisome forms, leading to the resumption of DNA replication.<sup>47,48</sup> Primosome assembly on ssDNA requires that PriA be bound to DNA and ATP only and does not require ATP hydrolysis.<sup>49</sup>

It is becoming increasingly clear that SSB plays important roles in rescuing stalled replication forks in addition to the binding of exposed ssDNA.<sup>50</sup> It binds to the fork in a polar fashion and performs limited unwinding.<sup>51</sup> SSB interacts functionally with Rep and UvrD to ensure that they do not process the same fork structure simultaneously.<sup>52</sup> The protein binds to both RecG and PriA *in vitro* and *in vivo*.<sup>3,38,42,43,53</sup> SSB also interacts functionally with RecG and separately with PriA.<sup>4,42,54</sup> One outcome of this interaction is to both regulate and stimulate the helicase activity of PriA.<sup>40,42</sup> To understand how this might occur, an atomic force microscopy (AFM) study was done so that potential interactions between SSB and PriA could be visualized directly.<sup>38</sup> As PriA is an ATPase, and to eliminate potential complications due to ATP binding and hydrolysis, this study was done in the absence of a nucleoside triphosphate. Results show that PriA binds preferentially to a

fork substrate with a 69 nt gap in the leading strand and then remains bound exclusively at the fork as it does not translocate in the absence of ATP. In contrast, fork-bound SSB loads PriA onto the duplex DNA arms of forks. This effect is significant as PriA does not normally bind to duplex DNA. Therefore, as SSB occluded the ssDNA binding site, the only way for the helicase to be loaded is if it was remodeled by SSB during the loading process so that duplex DNA-binding was enabled, similar to what was shown for RecG.<sup>38,53</sup> A follow-up AFM study has revealed that in the presence of ATP but in the absence of SSB, the interaction of PriA with forks is dynamic, with initial fork binding followed by translocation onto the dsDNA regions of substrates, up to a maximum distance of 400 bp away from the fork in the parental duplex region.<sup>55</sup> The direction of translocation by PriA was dictated by the polarity of the 69 nt ssDNA tail. This study also revealed the ability of PriA to change direction during translocation on dsDNA. Collectively, these AFM studies show that the fork structure, ATP, and SSB play key roles in influencing the interaction of PriA with forks, as suggested previously.<sup>2,40,45</sup> However, the mechanism for this collective effect on PriA is unknown.

To begin to understand the mechanism of these SSB enhancements, a detailed characterization of the ATPase activity of PriA was performed in the presence of forks, and the catalytic efficiency of PriA in the presence and absence of SSBs was determined. We extend the previous studies to show that while the 3'-OH group present at the fork on the nascent leading strand is required to activate the ATPase activity of the enzyme, it is essential for efficient ATP hydrolysis. The results also show that this group is not sufficient for maximum activity as this is only achieved in the presence of SSB. In the presence of this SSB, the ability of PriA to discriminate the correct fork is increased by as much as 140-fold relative to the incorrect forks. SSB achieves this by modulating the affinity of PriA for both ATP and DNA, as well as the catalytic efficiency of the ATPase activity of the enzyme. Regulation of the ATPase activity of PriA, in addition to regulating the helicase activity of the enzyme, is critical as there are a very small number of PriA molecules available in the cell and it is essential that the helicase does not mistakenly load on the incorrect strand or structure, and SSB ensures this does not happen. The outcome

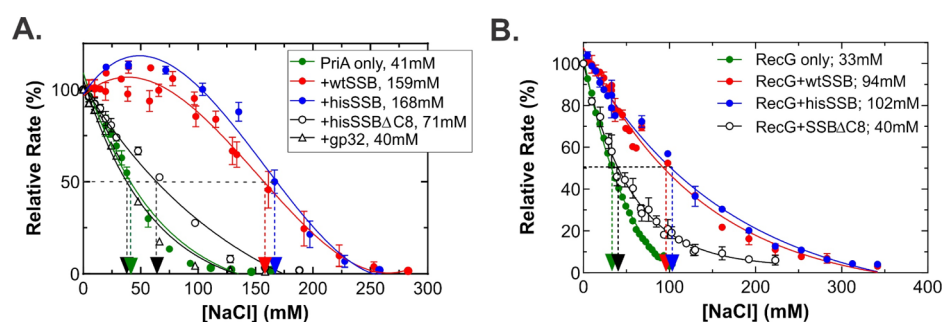


**Figure 2.** *E. coli* SSB stabilizes fork rescue DNA helicases on ssDNA. (A) Stabilization of PriA on  $\phi$ X174 ssDNA and (B) stabilization of RecG on M13 ssDNA. Assays were done as described in the [Materials and Methods](#) and contained 10 mM magnesium acetate (MgOAc), 1 mM ATP, 10  $\mu$ M nucleotides of ssDNA, 20 nM PriA or 10 nM RecG, and 1  $\mu$ M SSB (where indicated). To obtain the STMP, the resulting rates of ATP hydrolysis at each concentration of NaCl were calculated during each phase of the reaction following the addition of NaCl and expressed as a percent of the reaction rate in the absence of added NaCl. The dashed lines indicate the STMP for each reaction. A minimum of four separate assays was done for each reaction condition. The STMP data for RecG have been published earlier, but assays were redone, and the resulting data are presented here for direct comparison to PriA.<sup>3,4</sup>

is that replication restart is directed to only the template lagging strand.

## RESULTS

**PriA Exhibits Robust ATPase Activity on  $\phi$ X174 ssDNA That Is Stimulated by SSB.** The hydrolysis of ATP by PriA in the presence of various DNA molecules under several assay conditions was monitored utilizing a coupled spectrophotometric assay that we used previously to understand DNA substrate specificity for RecG, RuvAB, Rep, and UvrD.<sup>4,52,56</sup> We first analyzed the activity of PriA on ssDNA using M13 as the cofactor which is the standard for most of our helicase studies.<sup>4,52</sup> The activity of PriA in the presence of this ssDNA was very low at  $3.7 \pm 0.8 \mu\text{M}/\text{min}$  (Figure 1A). Furthermore, a stoichiometric amount of SSB inhibits the ATPase activity of the protein by 4-fold in the presence of this DNA cofactor. Both findings are consistent with previous studies, but the magnitude of the effects observed here is greater.<sup>1,2</sup> In contrast, SSB enhances the ATPase activity of RecG in the presence of M13 ssDNA.<sup>4</sup>

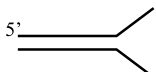
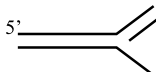
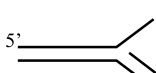
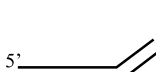

PriA was initially identified as a factor bound to a DNA hairpin structure in  $\phi$ X174 called PAS, leading to the subsequent assembly of the primosome, a complex responsible for primer RNA synthesis and duplex DNA unwinding at a replication fork.<sup>16,20,21</sup> Therefore, we tested the ATPase activity of the helicase in the presence of  $\phi$ X174 ssDNA. Consistent with previous work, the results show that the activity was 4-fold higher than that in the presence of M13 ssDNA (Figure 1A and refs 1 and 2). The higher level of activity of PriA in the presence of  $\phi$ X174 ssDNA is consistent with the helicase being a site-specific (i.e., PAS), structure-specific, and ssDNA-dependent ATPase.<sup>21,39</sup> Here, the enzyme recognizes PAS and then translocates on the ssDNA, concomitant with the hydrolysis of ATP. Furthermore, the ATPase activity of PriA is enhanced 2-fold by the SSB, in contrast to the inhibition reported previously.<sup>1</sup> In the previous work, a moderate stimulation (1.12-fold) was observed at low concentrations of SSB and activity was inhibited 35% at higher concentrations. Thus, the difference between our work and theirs may be due to differences in the concentration of SSB or PriA, although this was not provided in Shlomai and Kornberg.<sup>1</sup> Regardless, when compared to the SSB-containing reaction in the presence of M13 ssDNA, the ATPase activity of PriA is found to be stimulated 32-fold.

To determine whether the stimulation is specific to wild-type *Escherichia coli* SSB, assays were repeated using different SSBs in the presence of  $\phi$ X174 ssDNA. The results show that the T4 gene 32 protein will partially substitute for SSB, as it is only 78% as effective (Figure 1B; 21 vs 27  $\mu\text{M}/\text{min}$ , respectively). Second, the N-terminal histidine tag on SSB (his-SSB) reduces the enhancement by 30% to 18  $\mu\text{M}/\text{min}$  but still stimulates the activity of the enzyme. Finally, there is a small but noticeable stimulation (16  $\mu\text{M}/\text{min}$ ) provided by SSB $\Delta$ C8, a mutant SSB that lacks the last eight residues but has a wild-type linker domain required for partner protein binding.<sup>44,57,58</sup> As PriA and SSB interact physically and functionally, the result obtained with SSB $\Delta$ C8 indicates that, in this assay, the mutant retains 85% of this interaction (compare his-SSB to his-SSB $\Delta$ C8). Collectively, these data suggest that there are two components of the stimulation of the helicase afforded by a SSB: ssDNA (78%) and PriA binding (22%).

**SSB Stabilizes PriA on  $\phi$ X174 ssDNA.** Previous work has shown that SSB stabilizes the RecG on M13 ssDNA.<sup>4</sup> This stabilization was observed as a 2-fold increase in the salt-titration midpoint (STMP). To test if SSB has a similar effect on PriA, increasing amounts of sodium chloride (NaCl) were added to ongoing ATPase assays using  $\phi$ X174 ssDNA as the DNA cofactor. To permit a direct comparison to our published work, assays with RecG were repeated on the same day using the same assay components except that M13 ssDNA was employed as the cofactor.

The results show that the STMP for PriA alone was 41 mM and this increased 4-fold to 159 and 168 mM in the presence of wild-type and his-SSB, respectively (Figure 2A). SSB $\Delta$ C8 produced a 1.7-fold increase in the STMP indicating that it also stabilizes the helicase on ssDNA. In contrast, the bacteriophage T4 gene 32 protein (gp32) does not affect the STMP. As expected, SSB also stabilizes RecG on ssDNA, producing a 2.8-fold increase in the STMP (Figure 2B). In contrast to PriA, SSB $\Delta$ C8 had only a small but detectable effect on RecG. Therefore, SSB stabilizes both PriA and RecG on their respective ssDNA cofactors. The data also suggest that SSB–PriA interactions are important for this stabilization as both wild-type and SSB $\Delta$ C8 stabilize the helicase on ssDNA. Furthermore, SSB also stabilizes PriA on forks producing a 1.4- to 1.7-fold increase in the STMP (Table S2).

Table 1. DNA Cofactors and Their Uses

DNA substrate and group <sup>a</sup>	Design	Use	Oligonucleotides used in construction
Fork 1 (group I)		mimics a stalled fork with ssDNA gaps in both strands	170 173
Fork 2 (group I)		mimics a stalled fork with an ssDNA gap in the lagging strand	170 171 173
Fork 3 (group I)		mimics a stalled fork with an ssDNA gap in the leading strand	170 173 172
Fork 4 (group II)		mimics a nascent, regressed fork structure	170 171 173 172
Fork 5 (Holliday Junction ; group II)		mimics a structure resulting from the continued regression of fork 4	170 345 173 346

<sup>a</sup>These DNA substrates were used previously in the analysis of RecG and RuvAB in refs. <sup>3,4,56</sup>

**SSB Affects the ATPase Activity of PriA in a Fork-Structure-Dependent Manner.** Previous work from several laboratories showed that SSB interacts with PriA both physically and functionally.<sup>2,25,38,42,43,54,59</sup> To understand the mechanism of these interactions at forks where PriA plays critical roles *in vivo*, we utilized a series of model fork substrates to characterize the ATPase activity of PriA. We previously used these forks to characterize the ATPase activity of other DNA helicases—RecG, RuvAB, Rep, and UvrD.<sup>4,52,56</sup>

These model forks, shown schematically in Table 1, are formed by annealing purified oligonucleotides to produce a fork with flayed ends (fork 1); a fork with a gap in the lagging strand arm, which also has a 3'-OH positioned at the fork on the leading strand arm (fork 2); a fork with a gap in the leading strand (fork 3); a fork with two duplex arms (fork 4); and finally a HJ (fork 5).

Forks 1–3, which contain one or more ssDNA arms, comprise group I and are thought to mimic nascent, stalled replication fork structures. Fork 4 and the HJ, which contain duplex DNA arms, are assigned to group II as they are thought to mimic regressed fork structures. These last two forks were included initially to permit a comparison with RecG and RuvAB; even though PriA does bind to them it will not unwind them unless they contain a 5 nt gap at the fork.<sup>2,4,30,40,56</sup> At the center of each fork is a homologous core of 12 bp flanked by heterologous sequences so that similar to RecG, PriA can, in principle, mediate the unwinding of each of the substrates (data not shown<sup>60–62</sup>).

Previous studies of DNA helicase activity were done using model HJs and stalled fork substrates which themselves are influenced by magnesium ion concentration and could affect the resulting activity of PriA accordingly.<sup>4,52,63–67</sup> Therefore, to understand the mechanism of PriA interactions at forks, we first assessed the ATPase activity of the helicase as a function of magnesium ion concentration (Figure 3A, PriA only for schematic and B for the data). Results show that the activity of

PriA was maximal between 1 and 5 mM concentrations, with activity decreasing as the magnesium ion concentration was increased. The highest level of activity was observed in the presence of 1 mM MgOAc for fork 2. This is followed by fork 1 which has two single-stranded arms and an optimum also at 1 mM concentration. The ATPase activity of PriA decreased further when fork arms were duplex in character (fork 4 and the HJ). In addition, the magnesium ion optimum also changed to 2–4 mM. Extremely low levels of activity were observed in the presence of fork 3, which mimics a fork with a gap in the nascent leading strand. For this fork, the ATPase activity was 13-fold lower than that of fork 2, even at the optimal concentration of 1 mM MgOAc. The activity observed in the presence of fork 4 and the Holiday Junction was surprising. Fork 4 does have a 3'-OH group at the fork, but when the nascent lagging strand is present without a gap in this strand, inhibition relative to fork 2 occurs, similar to fork 3.<sup>45</sup> For the HJ, the absence of a 3'-OH at the fork and all four duplex arms resulted in a maximum level of ATPase activity that was only 2-fold lower than that of fork 2 (Figure 3B). This may be due to the ability of the HJ to adopt a bent, stacked X-structure configuration in the presence of magnesium ions that enables PriA binding.<sup>30,68</sup> Fork 4 and the HJ were not studied further as SSB is likely not involved in the initial binding of these DNA molecules to PriA.

To understand how SSBs influence the ATPase activity of PriA in the presence of forks with single-strand character, MgOAc titrations were repeated but in the presence of SSB, and the data were compared to those obtained for PriA alone (see Figure 3A for the schematic and Figure B–F for data). For fork 1, which has 2 ssDNA arms, the presence of SSB virtually eliminated the ATPase activity of PriA (Figure 3C). The inhibition seen here is greater than the 4-fold effect seen previously, and this may be due to the higher concentration of SSB relative to DNA used here.<sup>40</sup> Furthermore, inhibition was independent of whether SSB (200 nM tetramer) was added to

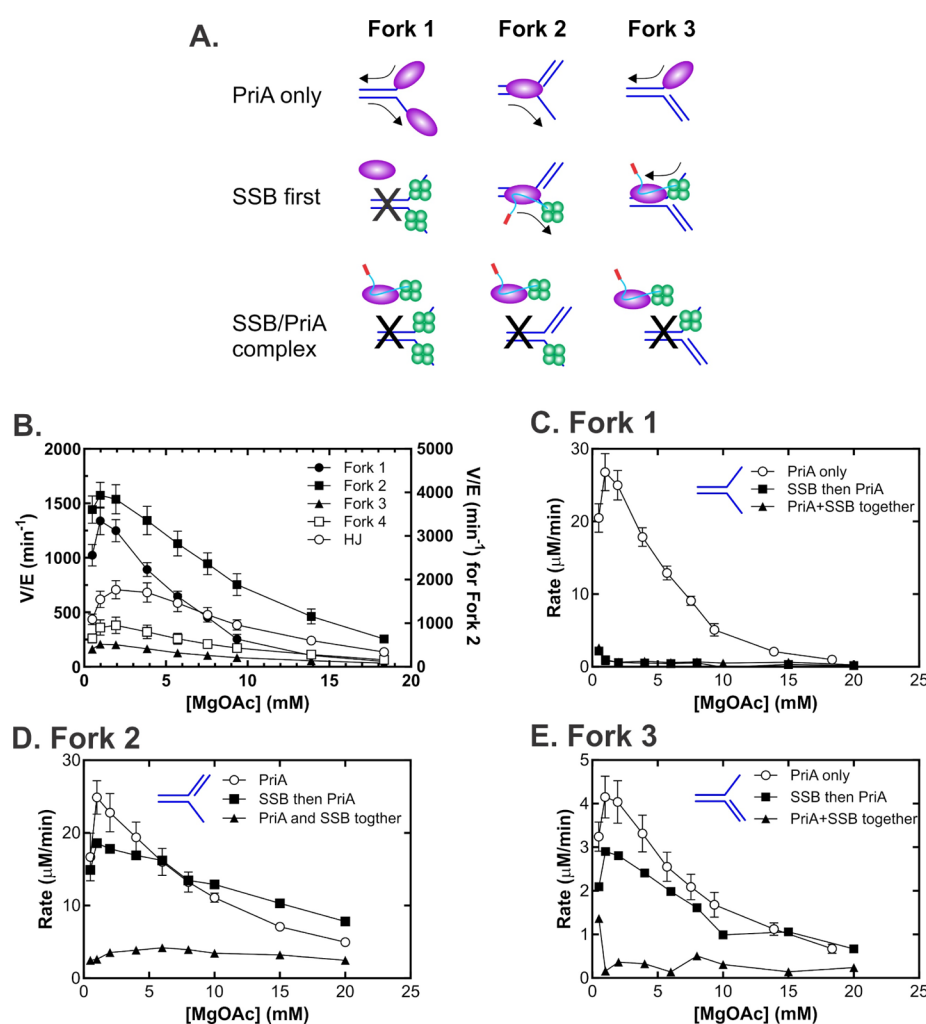


**Figure 3.** The order of addition dictates the effects of SSB on PriA in the presence of stalled fork DNA cofactors. (A) Schematic of the assay. Black arrows indicate the direction of translocation of PriA when bound to DNA. The black “X” indicates that activity is inhibited. Where SSB binds to PriA, the linker (light blue) and acidic tip (red) are shown for only the interacting monomer in the tetramer. (B–E) MgOAc titrations were done using fork cofactors as indicated. Assays contained 10 nM PriA helicase, 1 mM ATP, 100 nM molecules of each DNA cofactor, and either 200 nM (fork 1) or 100 nM (forks 2 and 3) SSB tetramer. (B) The magnesium optimum for PriA is fork-structure-dependent. (C) SSB inhibits the ATPase activity of PriA in the presence of a fork with two single-stranded tails. (D and E) When added first, SSB does not inhibit PriA in the presence of forks with a gap in the nascent lagging (D) or leading strands (E).

the forks first or allowed to bind to PriA (10 nM) before being added to the reaction. Also, inhibition was specific to *E. coli* SSB, with wild type having the greatest effect on PriA (Figure S1A). Even SSB $\Delta$ C8, which has mutant C-termini, is effective in inhibiting the ATPase activity of PriA on fork 1. In contrast, gp32, which binds to ssDNA with a polarity opposite to that of SSB and is not known to bind PriA, stimulates the ATPase activity of PriA on fork 1.<sup>51</sup>

In contrast to fork 1, SSB (100 nM tetramer) when added to fork 2 or 3 before PriA, had only a minimal effect on the ATPase activity of the helicase at the magnesium optimum (Figure 3D,E). Surprisingly, when PriA and SSB were premixed, ATPase activity in the presence of forks 2 and 3 was inhibited several-fold, independent of the concentration of MgOAc. This was specific to wild-type SSB for fork 2 and occurred with all SSBs tested for fork 3 (Figure S1). In summary, the data in this section show that when added separately, SSB stimulates the ATPase activity of PriA on fork 2, while it inhibits the ATPase activity of PriA on forks 1 and 3.

Previous work has shown that in the presence of forks, RuvAB is inhibited by SSB and the UvrD and Rep DNA helicases are destabilized, that is, their STMPs are decreased 2- to 5-fold.<sup>52,56</sup> In contrast, SSB stabilizes RecG in the presence of model forks.<sup>56</sup> This stabilization was observed as a 2-fold increase in the STMP for forks 1 and 3 and a 4-fold increase for fork 2. To determine the effect of SSB on the STMP of PriA in the presence of fork DNA, NaCl was added in small amounts in a successive fashion to separate, ongoing ATPase assays using forks 1 and 2. Fork 3 could not be studied as the rates of ATP hydrolysis are too low to be reliable. The results show that the STMP for PriA only was  $108 \pm 5$  mM in the presence of fork 2, and this is 2-fold higher than that obtained for fork 1 ( $49 \pm 6$  mM Table S2). SSB increased the STMP of PriA in the presence of fork 1, by 1.7-fold to  $85 \pm 6$  mM, and in the presence of fork 2, it increased 1.4-fold to  $149 \pm 1$  mM. Collectively, these results show that the interaction of PriA with forks is stabilized by SSB, similar to that observed for  $\phi$ X174 ssDNA (Figure 2). Furthermore, the interaction of PriA alone with fork 2 is more stable as indicated by the 2-fold

Table 2. ATP Kinetic Parameters for PriA<sup>a</sup>

proteins present	DNA	$K_m^{\text{ATP}}$ ( $\mu\text{M}$ )	$V_{\text{max}}$ ( $\mu\text{M}/\text{min}$ )	$k_{\text{cat}}$ ( $\text{min}^{-1}$ )	$k_{\text{cat}}/K_m$ ( $\text{min}^{-1}/\text{nM}$ )
PriA	fork 1	2740 $\pm$ 936	8.1 $\pm$ 1.3	810	0.3
	fork 2	882 $\pm$ 232	16.9 $\pm$ 1.5	1690	1.9
	fork 3	1123 $\pm$ 635	2.2 $\pm$ 0.3	220	0.2
PriA + SSB	fork 1	1303 $\pm$ 551	43 $\pm$ 5.6	4300	3.3
	fork 2	852 $\pm$ 158	144 $\pm$ 10	14,400	16.9
	fork 3	1814 $\pm$ 884	5.1 $\pm$ 0.7	510	0.3
PriA + SSB $\Delta$ C8	fork 1	1871 $\pm$ 664	81 $\pm$ 13	8100	4.3
	fork 2	1733 $\pm$ 729	67 $\pm$ 13	6700	3.9
	fork 3	4540 $\pm$ 1,077	31 $\pm$ 4	3100	0.7
PriA + T4 gp32	fork 1	4,065 $\pm$ 1,256	144 $\pm$ 21	14,400	3.5
	fork 2	6,479 $\pm$ 2,283	110 $\pm$ 22	11,000	1.7
	fork 3	2677 $\pm$ 2051	15 $\pm$ 2	1500	0.6

<sup>a</sup>Assays were done as described in the Materials and Methods. The data were approximated by the Michaelis–Menten equation.

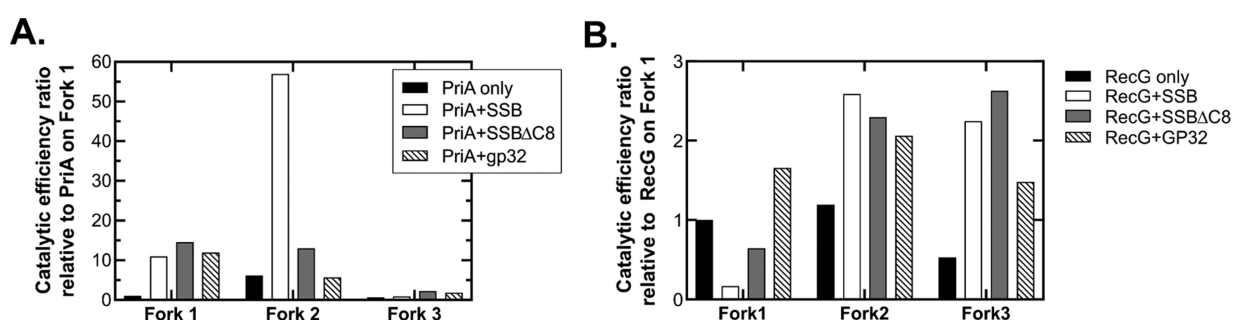


**Figure 4.** Wild-type *E. coli* SSB enhances fork-substrate discrimination by PriA. To enable direct comparison, the data in each panel have been normalized to the catalytic efficiency for the ATPase activity of each helicase alone in the presence of fork 1. Kinetic data were obtained from ATPase assays and are shown in a graph format in Figure S2 for PriA (not shown for RecG). The values are presented in Table 2 and were used to calculate the ratios presented. (A) Wild-type SSB specifically increases the catalytic efficiency of PriA in the presence of fork 2, its preferred fork cofactor. (B) SSB has minimal effects on the catalytic efficiency of RecG. Assays with each fork were done as ATP titrations in the absence and presence of SSBs.

higher STMP relative to fork 1. This is consistent with this fork being the preferred DNA substrate for PriA.

**ATP Titrations Reveal an Insight into How SSB Regulates PriA Activity at Forks.** To further understand how SSBs influence the activity of DNA helicase at a fork, we performed ATP titrations and determined the relevant kinetic parameters for PriA. Assays were done in the presence of forks 1–3 and were done with PriA only, and separately in the presence of either SSB, SSB $\Delta$ C8, or gp32. The raw data are shown in Figure S2, kinetic parameters are presented in Table 2 and the final analysis is shown in Figure 4.

First, an inspection of the curves in Figure S2A shows that under these assay conditions, the preferred fork substrate is fork 2 which has a gap in the nascent lagging strand and the requisite 3'-OH group in the nascent leading strand, consistent with previous works.<sup>33,40,69</sup> Second, SSB increases the  $V_{\text{max}}$  of PriA in the presence of forks 1–3 by 5-, 9-, and 2.3-fold, respectively (Figure S2B, and for precise numbers, see Table S2). This is accompanied by a decrease in the  $K_m^{\text{ATP}}$  for fork 1 and an increase for fork 3, while in the presence of fork 2,  $K_m^{\text{ATP}}$  is unaffected. Third, SSB $\Delta$ C8 also increases the  $V_{\text{max}}$  of PriA by 10-fold on fork 1, 14-fold on fork 3, and only 4-fold on fork 2, but it also increases the  $K_m^{\text{ATP}}$  relative to SSB for each fork (Figure S2C and Table S2). Fourth, gp32 also stimulates the  $V_{\text{max}}$  of PriA in the presence of forks, but this is accompanied by a 2- to 8-fold increase in the  $K_m^{\text{ATP}}$  (Figure S2D and Table S2).

To further understand the mechanism of these SSB- and fork-specific stimulations, kinetic parameters were calculated and the catalytic efficiency of the helicase assessed (Table 2). First, the catalytic efficiency of PriA alone in the presence of fork 2 is 1.9, which is 6- to 10-fold higher than forks 1 and 3, respectively (Table 2). The high catalytic efficiency observed for fork 2 is a combination of high  $V_{\text{max}}$  and the lowest  $K_m^{\text{ATP}}$  among the three forks.

In the presence of SSB, the catalytic efficiency of PriA changes dramatically. First, it increases 9-fold on fork 2, 10-fold on fork 1, and is unchanged on fork 3, relative to PriA alone on these same forks (Table 2). However, the  $k_{\text{cat}}/K_m^{\text{ATP}}$  for fork 2 in the presence of SSB is 5- to 56-fold higher than forks 1 and 3, respectively. This is attributed to an 8-fold increase in  $V_{\text{max}}$  as the  $K_m^{\text{ATP}}$  was unaffected. SSB $\Delta$ C8 also increases the catalytic efficiency of PriA in the presence of each fork, relative to PriA alone. However, the increase observed for fork 1 is the same as that of SSB; for fork 2, it is 4-fold lower, and while there is a stimulation for fork 3, it is still 6-fold lower than the other forks. SSB $\Delta$ C8 produces these effects by impacting both the  $V_{\text{max}}$  and the  $K_m^{\text{ATP}}$  in a fork-dependent manner. For fork 1, when compared to SSB, both parameters increase; for fork 2,  $V_{\text{max}}$  decreases, and this is accompanied by a 2-fold decrease in the affinity for ATP; for fork 3, the increase in  $V_{\text{max}}$  is accompanied by a 2.5-fold increase in the  $K_m^{\text{ATP}}$ . Finally, T4 gp32 also increases the catalytic efficiency of PriA to the same extent as observed for SSB and SSB $\Delta$ C8 in the presence of forks 1 and 3 but has no effect in the presence of fork 2. The

Table 3. Kinetic DNA Parameters for PriA<sup>a</sup>

DNA	$K_m^{\text{app}}$ (nM)	$V_{\text{max}}$ ( $\mu\text{M}/\text{min}$ )	$k_{\text{cat}}$ ( $\text{min}^{-1}$ )	$k_{\text{cat}}/K_m^{\text{app}}$ ( $\text{min}^{-1}/\text{nM}$ )	Hill coefficient
fork 1	5.7 ± 0.7	3.6 ± 0.1	1800	316	1.2 ± 0.1
fork 1 + SSB	13.4 ± 3.3	3.3 ± 0.2	1650	124	1.0
fork 2	6.8 ± 0.5	7.3 ± 0.2	3650	537	2.1 ± 0.3
fork 2 + SSB	5.3 ± 0.7	4.5 ± 0.1	2250	424	1.0
fork 3 <sup>b</sup>	17 ± 7	0.6 ± 0.04	300	18	1.9 ± 0.5
fork 3+SSB	ND <sup>c</sup>	ND			

<sup>a</sup>Assays were done as described in the Materials and Methods. The data were approximated by the Hill equation. <sup>b</sup>Substrate inhibition is observed for this DNA. Using the limited amount of data, kinetic parameters were calculated, but they should be viewed with caution. See Figure S3. <sup>c</sup>ND, not done.

increase seen here is attributed to a large jump in  $V_{\text{max}}$  but this is offset by the 2–8-fold increase in the  $K_m^{\text{ATP}}$ . In summary, each SSB affects the ATPase activity of PriA in a fork-dependent manner. The effectiveness of the proteins is ranked as SSB > SSBΔC8 > gp32. The largest stimulation in catalytic efficiency is seen for SSB in the presence of fork 2.

The presence of the 3'-OH group on the nascent leading strand in fork 2 results in the highest catalytic efficiency of PriA alone. SSB increases both the STMP of PriA on this fork and produces the maximal increase in  $k_{\text{cat}}/K_m^{\text{ATP}}$ . Therefore, to understand the combined effect of both the 3'-OH group and SSB, we normalized the catalytic efficiency data to that of PriA only in the presence of fork 1 (no 3'-OH group and no SSB). When analyzed in this manner, the combined effect increases the catalytic efficiency of PriA by 56-fold in the presence of fork 2 (Figure 4A). As any SSB increases the  $k_{\text{cat}}/K_m^{\text{ATP}}$  in the presence of fork 1, the effect of ssDNA binding by these proteins on the helicase can be observed. This can also be seen for fork 2, where not only the effect of ssDNA binding is seen (SSBΔC8 vs PriA alone) but also the effects of polarity (gp32 inhibits, whereas SSB and SSBΔC8 stimulate). In the presence of fork 3, the effects of a SSB are negated by the nascent lagging strand. The presence of the nascent lagging strand results in a fork that is unfavorable for PriA. Consequently, the enhancement in catalytic efficiency observed for PriA in the presence of fork 2 and SSB, relative to PriA alone in the presence of fork 3 is 84.5-fold (no 3'-OH and an inhibitory nascent lagging strand).

In contrast to PriA, the effects of SSBs on the catalytic efficiency of RecG are at best moderate (Figure 4B). SSB does, however, decrease the catalytic efficiency of RecG in the presence of fork 1 while increasing this kinetic parameter 2-fold for fork 2 and 5-fold for fork 3 (the preferred fork substrate for this enzyme<sup>4,56</sup>). However, comparable effects are also observed for SSBΔC8 and gp32 indicating that the presence of a SSB enhances the catalytic efficiency of RecG but does not facilitate further substrate discrimination. These data are consistent with a special and unique interaction between SSB and PriA that does not apply to RecG.

**Analysis of DNA Kinetic Parameters Confirms the DNA Cofactor Specificity.** To determine whether SSB influences the binding specificity of PriA for fork substrates, ATPase assays were repeated, but this time the concentration of DNA was varied and kinetic parameters were calculated. The results show that as anticipated, the preferred cofactor is fork 2 as the catalytic efficiency of the enzyme is highest in the presence of this DNA (Table 3). It was 1.7-fold higher than that observed for fork 1 and 30-fold higher than that observed for fork 3. We note cofactor inhibition for fork 3 (Figure S3). Furthermore, for fork 2, a Hill coefficient of  $2.1 \pm 0.3$  was

observed suggesting that under these conditions, PriA can bind at least two of these forks resulting in high levels of activity. The values for  $K_m^{\text{app,DNA}}$  obtained here are comparable to the  $K_d$  values reportedly previously for comparable fork substrates.<sup>30,33</sup>

When assays were done in the presence of stoichiometric SSB relative to forks, several changes in the kinetic parameters of PriA were observed. First, the Hill coefficient for DNA binding for each fork was 1. Second, the catalytic efficiency of the enzyme in the presence of fork 1 decreased 2.5-fold. This is attributed to a 2-fold decrease in the apparent affinity of the enzyme for this fork from  $5.7 \pm 0.7$  to  $13.4 \pm 3.3$  nM (Table 2). Thus, this is the third contribution to further enhancing substrate discrimination by PriA—lowering the apparent affinity for a DNA cofactor which is not ideal for replication restart. For fork 2, there was a 1.2-fold decrease in  $k_{\text{cat}}/K_m^{\text{app}}$  and this was due to the decrease in  $V_{\text{max}}$ . However, SSB still produced a 2-fold increase in the ability of PriA to discriminate between forks 2 and 1, due to the large difference in catalytic efficiency. Therefore, the combined effects of contributions of SSB on the ability of PriA to discriminate between forks is 140-fold. This value is obtained from the combined effects observed in the ATPase and DNA titrations ( $k_{\text{cat}}$  stimulation of 56-fold and  $K_m^{\text{DNA,app}}$  reduction of 2.5-fold).

## DISCUSSION

The primary conclusion of this study is that SSB facilitates fork discrimination by PriA by as much as 140-fold. SSB exerts these effects by regulating the affinity of the helicase for both ATP and DNA and by modulating the catalytic efficiency of the enzyme. The effects of SSB are the greatest in the presence of fork 2, which has a gap in the lagging strand and a 3'-OH group positioned at the fork on the nascent leading strand. The combination of these effects, that is, SSB, ATP hydrolysis, and the 3'-OH group, as well as the blocking of PriA binding to aberrant single strands of DNA exposed at forks and loading of the helicase onto the parental duplex in the right orientation, ensures that the preprimosome can be loaded onto the template lagging strand and that replication restart proceeds in the correct direction.

PriA is an unusual DNA helicase with unique DNA-binding specificity that is in some respects similar to RecG but very distinct in its own right.<sup>4,26,56,70</sup> RecG binds to D-loops and prefers a fork with a gap in the nascent leading strand. PriA also binds to D-loops and model fork structures but demonstrates a preference for a fork with a gap in the nascent lagging strand.<sup>2,24,25,30–32,40,71</sup> It was later shown that the enzyme has a 3'-terminus binding pocket that plays a key role in facilitating specific binding to a fork when this 3'-OH is positioned on the nascent leading strand at the fork producing

a  $K_d = 1\text{--}2\text{ nM}$ .<sup>33,34</sup> This binding is also critical to the activation of the ATPase activity.<sup>32</sup> When this 3'-OH group is absent or blocked by the addition of a phosphate group,  $K_d$  increases 8- to 10-fold, and while ATPase activity is still observed, it is reduced to a 5-fold lower level. We now show that this 3'-OH group positioned at the fork is also required for efficient ATPase activity of PriA (Figures 3, 4, and Table 2). This group enhances the catalytic efficiency of the enzyme 6-fold relative to forks where it is absent. This results from a 3-fold lower  $K_m^{\text{ATP}}$  and a 2-fold higher  $V_{\text{max}}$  in kinetic assays (Tables 2 and 3). The presence of the nascent lagging strand inhibits the helicase and ATPase activities of PriA, with ATP hydrolysis (not binding) facilitating the ability of the helicase to discriminate fork substrates, consistent with previous proposals.<sup>40,45</sup> In fact, the work of Manhart demonstrates that the ability to hydrolyze ATP by PriA is critical for fork substrate discrimination as this activity is absent in PriA K230R which cannot hydrolyze ATP,<sup>45</sup> but that is not all. The results herein show that SSB is also a key component in determining how PriA processes forks.

The sum of the combined 3'-OH/SSB effect is a 140-fold increase in the ability of PriA to discriminate the correct fork from the incorrect one. SSB introduces two components for catalytic efficiency enhancement. First, there is polar ssDNA binding of SSB to the template lagging strand, and second, there is an interaction between the SSB and PriA that involves linker/OB-fold binding.<sup>44,51</sup> The binding of SSB to the lagging strand also blocks access to this ssDNA by PriA. This makes sense because PriA binds to ssDNA with high affinity, so if it binds to the lagging strand template, it will translocate away from the fork in the 3'-5' direction.<sup>30,32</sup> Instead, and second, the lagging strand-SSB binds directly to PriA and loads the remodeled enzyme onto the parental duplex DNA.<sup>38</sup> This is a fundamental change in PriA as the helicase does not normally bind to dsDNA.<sup>30,38</sup> In the process, SSB ensures that only one PriA binds to the fork (Hill coefficient for DNA binding changes from 2 to 1); it alters the affinity of the helicase for DNA (Table 3) and impacts the ATPase kinetics of PriA. For fork 2, which is the preferred fork, activity is significantly enhanced. For forks 1 and 3, the activity of PriA is essentially shut down, presumably because SSB has coated PriA-binding sites and is preventing the helicase from interacting with the fork as suggested previously.<sup>45</sup> This also eliminates the checkpoint activity of the helicase on these fork substrates.<sup>45</sup> We note that T4 gp32 and SSB $\Delta$ C8 also impact the ATPase activity of PriA, but when compared to SSB, they inhibit the helicase on most forks, largely by decreasing the affinity of the enzyme for ATP (Table 2).

SSB, in addition to enhancing substrate discrimination by PriA and regulating the checkpoint function, also stabilizes the enzyme on the DNA, as evidenced by the increases in the STMP in the presence of either forks or  $\phi$ X174. This indicates that once loaded and fork recognition occurs, translocation and unwinding ensue with PriA tracking on the template lagging strand. SSB binds to ssDNA with high affinity and approximately 10 pN of force is required to displace a single tetramer.<sup>72,73</sup> However, it does not represent an impassable block to the translocating helicase, which displaces SSB (Figures 1, 2, and ref 1). Thus, like RecG, SSB loads PriA onto the DNA and is then subsequently displaced during translocation by the helicase.<sup>38,53,74,75</sup>

In exponentially growing cells, there are more than 2000 SSB tetramers per cell.<sup>76</sup> In these same cells, there are on

average 2-4 DNA replication forks per cell with as many as 25 tetramers bound per fork. At each fork, there is 0.5-1 kb of ssDNA available.<sup>77</sup> Using a site size of 40 nucleotides occluded per tetramer, there would be on average 25 tetramers bound per fork or 100 per cell with the free SSB localizing to the inner membrane.<sup>78</sup> In contrast to SSB, the levels of PriA are significantly lower at 2-4 molecules per cell.<sup>76</sup> By binding to SSB, PriA also localizes to the inner membrane in the absence of exogenous DNA damage.<sup>43</sup> When forks stall, PriA must be transferred to the DNA. However, results herein show that premixing SSB and PriA before binding to the DNA reduces the activity of PriA at forks (Figure 3B-D). This suggests that PriA must be transferred from the storage form complex to the SSB already bound at the fork. The mechanism for this is unknown but could involve SSB to SSB transfer. Once there, SSB plays its important role in remodeling PriA, loading the enzyme onto duplex arms, and enhancing the catalytic function of the helicase so that its ability to discriminate the correct fork substrate from the incorrect one in the presence of ATP is enhanced 140-fold. Thus, while ATP hydrolysis is not required for the replisome assembly on ssDNA, it is required to recognize the correct fork, then process that fork, and displace both SSB and a sufficient amount of the nascent lagging strand if present, so that the replisome can be reloaded.<sup>32,35,45,49</sup>

The results herein also provide an insight into the timing of the interaction of PriA with forks. It is known that RecG regresses forks into structures with duplex arms (fork 4 in this study), as well as HJs.<sup>69,74</sup> As both the ATPase and helicase activities of PriA are inhibited on fork 4, and as SSB plays a critical role in facilitating the activity of the enzyme on forks with single-strand DNA character, these data suggest that PriA does not act on regressed forks. Instead, and as RecG and PriA have different fork specificities, the results indicate that PriA processes stalled forks with a gap in the nascent lagging strand and RecG, forks with either a gap in the nascent leading strand or forks with duplex arms. When RecG remodels its preferred fork, a HH is produced, with further processing required to reload the replisome. In contrast, when PriA remodels its preferred fork, the replisome can be reloaded directly onto the exposed ssDNA of the template-lagging-strand arm without the requirement for further processing.

Due to the very small number of PriA molecules available in the cell, it is essential that a mistake not be made. SSB ensures that this will not happen and, ultimately, the properly positioned PriA loads the preprimosome onto the correct strand at the fork (i.e., the template-lagging strand) so that the resumption of DNA replication proceeds in the right direction.<sup>45</sup> The effects of SSB on PriA presented herein are consistent with the protein's role in affecting the outcome of events at a fork, as shown previously for RuvAB, Rep, UvrD, and RecG.<sup>3,44,52,53,56</sup>

## ■ MATERIALS AND METHODS

**Materials.** All chemicals were of reagent grade, made up in Nanopure water, and passed through 0.2  $\mu\text{m}$  pore size filters. Yeast extract and tryptone were from Becton Dickinson and Company (MD, USA). NaCl, sucrose, Tris base, KCl,  $\text{Na}_2\text{HPO}_4$ ,  $\text{NaH}_2\text{PO}_4$ , EDTA, acetic acid, methanol, and nickel sulfate were from J.T. Baker (NJ, USA). Ampicillin was from Fisher (NJ, USA). IPTG was from OmniPur (NJ, USA). Kanamycin, chloramphenicol, lysozyme, and sodium deoxycholate were from Sigma (MO, USA). Benzonase was from Novagen (NJ, USA). Imidazole was from EMD (NJ, USA).



Coomassie brilliant blue R-250 was from Bio-Rad Laboratories (CA, USA). Glucose was from Mallinckrodt (KY, USA). Nonidet P40 substitute was from USB (OH, USA). ATP and DEAE Sepharose Fast Flow (FF), Q-Sepharose, HisTrap FF, 16/10 heparin FF, Mono Q, and Mono S 5/50 GL columns were from GE Healthcare Life Sciences (NJ, USA). Phosphoenol pyruvate (PEP), nicotinamide adenine dinucleotide (NADH), pyruvate kinase (PK), lactate dehydrogenase (LDH), and ssDNA-cellulose resin were from Sigma. Phosphocellulose (P11) was from Whatman. Bio-Gel HTP hydroxyapatite was from Bio-Rad. Dithiothreitol (DTT) was from Acros Organics. BSA and *Hind*III were purchased from New England Biolabs. Wheat germ topoisomerase I (WGT) was from Promega.

**Reagents.** All solutions were prepared using Barnstead Nanopure water. Stock solutions of PEP were prepared in 0.5 M Tris-acetate (Tris-OAc; pH 7.5). ATP was dissolved as a concentrated stock in 0.5 M Tris-HCl (pH 7.5), with the concentration determined spectrophotometrically at  $\lambda = 259$  nm using an extinction coefficient of  $1.54 \times 10^5 \text{ M}^{-1} \text{ cm}^{-1}$ . NADH was dissolved in 10 mM Tris-OAc (pH 7.5), with the concentration determined using an extinction coefficient of  $6250 \text{ M}^{-1} \text{ cm}^{-1}$ , and stored in small aliquots at  $-80^\circ\text{C}$ . DTT was dissolved as a 1 M stock in Nanopure water and stored at  $-80^\circ\text{C}$ . All reaction buffers described below were assembled at 10 times reaction concentration and stored in 1 mL aliquots at  $-80^\circ\text{C}$ .

**DNA Cofactors.** For all DNA cofactors, the concentrations of stock solutions were determined in  $\mu\text{M}$  nucleotides using the extinction coefficients as indicated below. To permit direct comparisons between fork DNA cofactors, concentrations and subsequent  $K_m^{\text{DNA,app}}$  values are reported in nM molecules for all assays.

*M13 mp18 ssDNA* was prepared as described in ref 4. The concentration of DNA was determined spectrophotometrically using an extinction coefficient of  $8780 \text{ M}^{-1} \text{ cm}^{-1}$  (nucleotides). Purified DNA was stored in small aliquots at  $-80^\circ\text{C}$ .

$\phi\text{X174 ssDNA}$  was purchased from New England Biolabs. The concentration of DNA was determined spectrophotometrically using an extinction coefficient of  $8780 \text{ M}^{-1} \text{ cm}^{-1}$  (nucleotides). Following concentration determination, the ssDNA was distributed into small aliquots and stored at  $-80^\circ\text{C}$ .

*Model fork-DNA substrates* consisting of a homologous core of 12 bp flanked by heterologous duplex arms of 19–25 bp were constructed by annealing gel-purified oligonucleotides. The substrate design was identical to that used previously.<sup>4,56</sup> The junction point can branch-migrate within the homologous core, whereas the heterologous arms prevent the spontaneous resolution of the junction DNA (Supporting Information Table S1).

Model fork substrates were prepared by annealing six oligonucleotides in various combinations: PB170 (5'-CTAGAGACGCTG CCGAATTCTGGCTTGGATCTGATGCTGTCTAGAGGCTCCACTATGAAATCGCTGCA-3'), PB171 (5'-GCGATTTTCATAGTGGAGGCCTCTAGACAGCA-3'), PB172 (5'-TGCTGTCTAG AGACTATCGATCTATGAGCTCTGCAGC-3'), PB173 (5'-CCGGGCTGCAGAGCTCATAGA TCGATAGTCTTAGACAGCATCAGATCCAAGCCAGAATTCGGCAGCGTCT-3'), PB345 (5'-GCGATTTTCATAGTGAGGCCTCTAGACAGCACGCGTTGAATGGGCGGATGCTAATTACTATCTC), and PB346 5'-

GAGATAGTAATT AGCATCCGCCCATTCACCGGCGTGCTGTCTAGAGACTATCGATCTATGAGTCTGCAGC). Purified oligonucleotides (1–10  $\mu\text{M}$  molecules each in different annealing experiments) were annealed in a total volume of 50  $\mu\text{L}$  containing 10 mM Tris-HCl (pH 7.5) or 10 mM Tris-OAc (pH 7.5), 100 mM NaCl, and 10 mM MgOAc. Annealing involved incubation of the DNA-buffer mixture in thin-walled PCR tubes at  $100^\circ\text{C}$  for 5 min, followed by an overnight cooling step to room temperature. The extent of annealing was verified by non-denaturing PAGE using 5'-end labeled oligonucleotides annealed under identical conditions (data not shown). Typically, >95% of the DNA present was found to be in the annealed substrate (data not shown). Junctions were added directly to ATPase assays without further purification. Fork 1 was formed by annealing PB170 and 173 (at a ratio of 1:1.2); fork 2, by annealing PB170, 171, and 173 (at a ratio of 1:1.3:1.2); fork 3, by annealing PB170, 172, and 173 (at a ratio of 1:1.3:1.2); fork 4, by annealing PB170, 171, 172, and 173 (at a ratio of 1:1.3:1.3:1.2), and finally the HJ contained oligonucleotides obtained by annealing PB170, 173, 345, and 346 (at a ratio of 1:1.2:1.3:1.3) (Table 1). As the annealing reactions contained 10 mM MgOAc, the concentration of magnesium ions in each assay was adjusted accordingly.

**Proteins.** *RecG* (UniProt-KB P24230) was purified as described previously.<sup>56</sup> The protein concentration was determined spectrophotometrically using an extinction coefficient of  $49,500 \text{ M}^{-1} \text{ cm}^{-1}$ .<sup>79</sup> No contaminating nuclease activity was found in the purified protein (data not shown).

*His-PriA* (UniProt-KB P17888) cloning was done as described previously.<sup>43</sup> To lyse cells, a 1 L culture was grown at  $37^\circ\text{C}$  with protein expression induced by the addition of 500  $\mu\text{M}$  IPTG at an  $\text{OD}_{600}$  of 0.5, followed by growth for an additional 3 h at  $37^\circ\text{C}$ . Cells were harvested by centrifugation, and lysis of the resuspended cell pellet was initiated by the addition of lysozyme (1 mg/mL final), and benzonase (3  $\mu\text{L}$ ), followed by stirring for 30 min at  $4^\circ\text{C}$ . Deoxycholate was added to 0.05% final, and the mixture was stirred for additional 30 min. Imidazole and KCl were added to the final at concentrations of 30 and 600 mM, respectively. The whole-cell lysate was centrifuged at 37,000g at  $4^\circ\text{C}$  for 1 h. The cleared cell lysate was loaded onto a 5 mL HisTrap FF column equilibrated in binding buffer (30 mM imidazole, 15.4 mM  $\text{Na}_2\text{HPO}_4$ , 4.5 mM  $\text{NaH}_2\text{PO}_4$ , and 600 mM KCl; pH 7.4). The nickel column was subjected to three washes sequentially: binding buffer (50 column volume (CV)), binding buffer with 0.2% NP40 (40 CV), and binding Buffer (30 CV). Proteins were eluted using a linear, imidazole gradient (30–500 mM in the same buffer). Fractions containing PriA were identified by 12% SDS-PAGE, pooled, and dialyzed overnight in heparin column binding buffer (20 mM Tris-OAc, (pH 7.5), 0.1 mM EDTA, 1 mM DTT, 40 mM KCl, and 10% glycerol). The purified protein was free of contaminating nuclease activity (not shown).

The next day, the dialyzed protein was subjected to centrifugation at 10,000g for 10 min and the supernatant was applied to a 20 mL heparin FF column equilibrated in heparin column binding buffer. Following a wash to baseline, the protein was eluted with a linear gradient (10 column volumes) from 40 to 1000 mM KCl in the same buffer. Fractions containing PriA (and no detectable contaminants) were identified by SDS-PAGE, pooled, and dialyzed overnight against storage buffer (20 mM Tris-HCl, pH 7.5; 0.1 mM

EDTA, 1 mM DTT, 100 mM NaCl, and 50% glycerol). Protein concentration was determined spectrophotometrically using an extinction coefficient of  $104,850 \text{ M}^{-1} \text{ cm}^{-1}$ .<sup>79</sup> The presence of the N-terminal histidine tag did not alter the activities of the protein relative to the untagged version (data not shown).

SSB (UniProt-KB P0AGE0) was purified from strain K12 $\Delta$ H1 $\Delta$ trp as described in ref 80. The concentration of purified SSB was determined at 280 nm using  $\epsilon = 30,000 \text{ M}^{-1} \text{ cm}^{-1}$ . The site size of SSB was determined to be 10 nucleotides per monomer by monitoring the quenching of the intrinsic fluorescence of SSB that occurs on binding to ssDNA, as described in ref 81. His-SSB was purified as described previously.<sup>43</sup> His-SSB $\Delta$ C8 was purified as described in ref 75. Contaminating ATPase or nuclease activity was not detected in either SSB, his-SSB or His-SSB $\Delta$ C8 (data not shown).

gp32 (UniProt-KB P03695) was over-expressed and purified as described in refs 82 and 83. The concentration of purified gp32 was determined at 280 nm using  $\epsilon = 37,000 \text{ M}^{-1} \text{ cm}^{-1}$ .<sup>84</sup> The site size of gp32 was determined to be seven nucleotides per monomer by monitoring the quenching of the intrinsic fluorescence of gp32 that occurs on binding to ssDNA, as described in ref 84. The purified protein was free of contaminating ATP and nuclease activity (data not shown).

**ATP Hydrolysis Assay.** The hydrolysis of ATP was monitored using a coupled spectrophotometric assay.<sup>4,56</sup> The conversion of ATP to ADP and  $P_i$  is linked to the oxidation of NADH to  $\text{NAD}^+$  and was monitored as a decrease in absorbance at 340 nm. The standard reaction buffer contained 20 mM Tris-OAc (pH 7.5), 1 mM DTT, 0.3 mM NADH, 7.5 mM PEP, 20 U/mL pyruvate kinase, 20 U/mL lactate dehydrogenase, 10 nM PriA, 1 mM ATP, and 10 mM MgOAc (but varied according to the DNA cofactor present). The rate of ATP hydrolysis was calculated by multiplying the slope of a tangent drawn to linear portions of time courses by 159 (derived from the extinction coefficient of NADH;  $6.3 \times 10^3 \text{ M}^{-1} \text{ cm}^{-1}$ ).<sup>4</sup> In a typical reaction, close to 200 data points were used to draw a linear fit to the data to calculate reaction rates. In assays with SSB present, it was stoichiometric relative to the fork. For example, for 100 nM fork 1, 200 nM tetramer was required (one per ssDNA arm); for forks 2 and 3, only 100 nM tetramer was required. This amount of tetramer was determined in fluorescence quenching experiments as described in ref 81.

To obtain kinetic parameters, data were analyzed using non-linear curve fitting in Prism v 8.4.3 (GraphPad Software, LLC). DNA titration data were fit to the Hill equation ( $V = (V_{\text{max}} [\text{DNA}]^n) / ([S_{0.5}]^n + [\text{DNA}]^n)$ ) or the Michaelis–Menten equation ( $V = (V_{\text{max}} [\text{DNA}]) / (K_m + [\text{DNA}])$ ).<sup>85</sup> ATP titration data were fit to the Michaelis–Menten equation only. In situations where the binding appeared cooperative, a comparison was done in Prism to determine which model more accurately described the data. Here, models were compared using the comparison of fit function and models discriminated using both *F*-test and *P*-values. In the instances where the Hill equation more accurately described the data, *P* values < 0.0001 and high *F*-values were obtained (data not shown).

In salt-titration experiments, the same reaction buffers were used (see above). Reactions were initiated by the addition of either PriA or RecG following a 5 min incubation of all other components. When SSBs were present, they were added before

PriA or RecG at the concentrations indicated in figure legends. Once a steady-state rate of ATP hydrolysis was achieved, NaCl was added in 12.5 mM increments (1  $\mu\text{L}$  volumes). This was repeated until all ATP hydrolysis of either PriA or RecG ceased. The resulting hydrolysis rate in each steady-state region was calculated and expressed as a percent of the steady-state rate in the absence of NaCl. The total volume used to calculate the final concentration of NaCl was adjusted after each addition to correct for the additions themselves. A line of best fit was drawn for data points between each addition, to obtain the ATP hydrolysis rate after each salt increment. The average number of data points used to determine the reaction rate was 14. These rates were subsequently graphed to determine the concentration of NaCl resulting in a 50% reduction in the rate of ATP hydrolysis which corresponds to the STMP.

## ■ ASSOCIATED CONTENT

### Supporting Information

The Supporting Information is available free of charge at <https://pubs.acs.org/doi/10.1021/acsomega.1c00722>.

Possible fork configurations and their equilibrium, SSB stabilization of PriA on forks, STMP values, ATPase assay raw data, and DNA titrations (PDF)

### Accession Codes

Protein Accession ID numbers: RecG—UniProt-KB P24230. PriA—UniProt-KB P17888. SSB—UniProt-KB P0AGE0. gp32—UniProt-KB P03695.

## ■ AUTHOR INFORMATION

### Corresponding Author

Piero R. Bianco – Department of Pharmaceutical Sciences, College of Pharmacy, University of Nebraska Medical Center, Omaha, Nebraska 68198-6025, United States; [orcid.org/0000-0003-2974-7952](https://orcid.org/0000-0003-2974-7952); Email: [pbianco@unmc.edu](mailto:pbianco@unmc.edu)

### Author

Hui Yin Tan – Department of Pharmaceutical Sciences, College of Pharmacy, University of Nebraska Medical Center, Omaha, Nebraska 68198-6025, United States; Present Address: Department of Chemistry and Biochemistry, University of Notre Dame, South Bend, IN 46556.

Complete contact information is available at:

<https://pubs.acs.org/doi/10.1021/acsomega.1c00722>

### Author Contributions

H.Y.T. conducted the experiments. H.Y.T. and P.R.B. analyzed the data. P.R.B. and H.Y.T. wrote the manuscript.

### Funding

Funding for the Bianco Laboratory was supported by the NIH grant GM10056 to PRB.

### Notes

The authors declare no competing financial interest.

## ■ REFERENCES

- (1) Shlomai, J.; Kornberg, A. A prepriming DNA replication enzyme of *Escherichia coli*. II. Actions of protein n': a sequence-specific, DNA-dependent ATPase. *J. Biol. Chem.* **1980**, *255*, 6794–6798.
- (2) Jones, J. M.; Nakai, H. Duplex opening by primosome protein PriA for replisome assembly on a recombination intermediate. *J. Mol. Biol.* **1999**, *289*, 503–515.

- (3) Buss, J. A.; Kimura, Y.; Bianco, P. R. RecG interacts directly with SSB: implications for stalled replication fork regression. *Nucleic Acids Res.* **2008**, *36*, 7029–7042.
- (4) Slocum, S. L.; Buss, J. A.; Kimura, Y.; Bianco, P. R. Characterization of the ATPase activity of the Escherichia coli RecG protein reveals that the preferred cofactor is negatively supercoiled DNA. *J. Mol. Biol.* **2007**, *367*, 647–664.
- (5) Cox, M. M.; Goodman, M. F.; Kreuzer, K. N.; Sherratt, D. J.; Sandler, S. J.; Marians, K. J. The importance of repairing stalled replication forks. *Nature* **2000**, *404*, 37–41.
- (6) Mirkin, E. V.; Mirkin, S. M. Replication fork stalling at natural impediments. *Microbiol. Mol. Biol. Rev.* **2007**, *71*, 13–35.
- (7) Voineagu, I.; Narayanan, V.; Lobachev, K. S.; Mirkin, S. M. Replication stalling at unstable inverted repeats: interplay between DNA hairpins and fork stabilizing proteins. *Proc. Natl. Acad. Sci. U.S.A.* **2008**, *105*, 9936–9941.
- (8) Kreuzer, K. N. DNA damage responses in prokaryotes: regulating gene expression, modulating growth patterns, and manipulating replication forks. *Cold Spring Harbor Perspect. Biol.* **2013**, *5*, a012674.
- (9) Atkinson, J.; McGlynn, P. Replication fork reversal and the maintenance of genome stability. *Nucleic Acids Res.* **2009**, *37*, 3475–3492.
- (10) Delagoutte, E.; von Hippel, P. H. Helicase mechanisms and the coupling of helicases within macromolecular machines Part I: Structures and properties of isolated helicases. *Q. Rev. Biophys.* **2002**, *35*, 431–478.
- (11) Bianco, P. R. *DNA helicases, eLS*; JohnWiley & Sons, Ltd: Chichester, 2012.
- (12) Killoran, M. P.; Keck, J. L. Sit down, relax and unwind: structural insights into RecQ helicase mechanisms. *Nucleic Acids Res.* **2006**, *34*, 4098–4105.
- (13) West, S. C. Processing of recombination intermediates by the RuvABC proteins. *Annu. Rev. Genet.* **1997**, *31*, 213–244.
- (14) Bianco, P. R. I came to a fork in the DNA and there was RecG. *Prog. Biophys. Mol. Biol.* **2015**, *117*, 166–173.
- (15) Huang, Y.-H.; Huang, C.-Y. Structural insight into the DNA-binding mode of the primosomal proteins PriA, PriB, and DnaT. *BioMed Res. Int.* **2014**, *2014*, 195162.
- (16) Wickner, S.; Hurwitz, J. Association of phiX174 DNA-dependent ATPase activity with an Escherichia coli protein, replication factor Y, required for in vitro synthesis of phiX174 DNA. *Proc. Natl. Acad. Sci. U.S.A.* **1975**, *72*, 3342–3346.
- (17) Schekman, R.; Weiner, J. H.; Weiner, A.; Kornberg, A. Ten proteins required for conversion of phiX174 single-stranded DNA to duplex form in vitro. Resolution and reconstitution. *J. Biol. Chem.* **1975**, *250*, 5859–5865.
- (18) Minden, J. S.; Marians, K. J. Replication of pBR322 DNA in vitro with purified proteins. Requirement for topoisomerase I in the maintenance of template specificity. *J. Biol. Chem.* **1985**, *260*, 9316–9325.
- (19) Jones, J. M.; Nakai, H. The phi X174-type primosome promotes replisome assembly at the site of recombination in bacteriophage Mu transposition. *EMBO J.* **1997**, *16*, 6886–6895.
- (20) Lee, E. H.; Masai, H.; Allen, G. C., Jr.; Kornberg, A. The priA gene encoding the primosomal replicative n' protein of Escherichia coli. *Proc. Natl. Acad. Sci. U.S.A.* **1990**, *87*, 4620–4624.
- (21) Masai, H.; Arai, K. DnaA- and PriA-dependent primosomes: Two distinct replication complexes for replication of Escherichia coli chromosome. *Front. Biosci.* **1996**, *1*, d48–d58.
- (22) Zipursky, S. L.; Marians, K. J. Identification of two Escherichia coli factor Y effector sites near the origins of replication of the plasmids (ColE1 and pBR322). *Proc. Natl. Acad. Sci. U.S.A.* **1980**, *77*, 6521–6525.
- (23) Zipursky, S. L.; Marians, K. J. Escherichia coli factor Y sites of plasmid pBR322 can function as origins of DNA replication. *Proc. Natl. Acad. Sci. U.S.A.* **1981**, *78*, 6111–6115.
- (24) Tanaka, T.; Mizukoshi, T.; Taniyama, C.; Kohda, D.; Arai, K.-i.; Masai, H. DNA binding of PriA protein requires cooperation of the N-terminal D-loop/arrested-fork binding and C-terminal helicase domains. *J. Biol. Chem.* **2002**, *277*, 38062–38071.
- (25) Chen, H.-W.; North, S. H.; Nakai, H. Properties of the PriA helicase domain and its role in binding PriA to specific DNA structures. *J. Biol. Chem.* **2004**, *279*, 38503–38512.
- (26) Windgassen, T. A.; Leroux, M.; Satyshur, K. A.; Sandler, S. J.; Keck, J. L. Structure-specific DNA replication-fork recognition directs helicase and replication restart activities of the PriA helicase. *Proc. Natl. Acad. Sci. U.S.A.* **2018**, *115*, E9075–E9084.
- (27) Zavitz, K. H.; Marians, K. J. Helicase-deficient cysteine to glycine substitution mutants of Escherichia coli replication protein PriA retain single-stranded DNA-dependent ATPase activity. Zn<sup>2+</sup> stimulation of mutant PriA helicase and primosome assembly activities. *J. Biol. Chem.* **1993**, *268*, 4337–4346.
- (28) Masai, H.; Deneke, J.; Furui, Y.; Tanaka, T.; Arai, K.-I. Escherichia coli and Bacillus subtilis PriA proteins essential for recombination-dependent DNA replication: involvement of ATPase/helicase activity of PriA for inducible stable DNA replication. *Biochimie* **1999**, *81*, 847–857.
- (29) Liu, J.; Nurse, P.; Marians, K. J. The Ordered Assembly of the phiX174-type Primosome. *J. Biol. Chem.* **1996**, *271*, 15656–15661.
- (30) Nurse, P.; Liu, J.; Marians, K. J. Two modes of PriA binding to DNA. *J. Biol. Chem.* **1999**, *274*, 25026–25032.
- (31) McGlynn, P.; Al-Deib, A. A.; Liu, J.; Marians, K. J.; Lloyd, R. G. The DNA replication protein PriA and the recombination protein RecG bind D-loops. *J. Mol. Biol.* **1997**, *270*, 212–221.
- (32) Tanaka, T.; Mizukoshi, T.; Sasaki, K.; Kohda, D.; Masai, H. Escherichia coli PriA protein, two modes of DNA binding and activation of ATP hydrolysis. *J. Biol. Chem.* **2007**, *282*, 19917–19927.
- (33) Mizukoshi, T.; Tanaka, T.; Arai, K.-i.; Kohda, D.; Masai, H. A Critical Role of the 3' Terminus of Nascent DNA Chains in Recognition of Stalled Replication Forks. *J. Biol. Chem.* **2003**, *278*, 42234–42239.
- (34) Sasaki, K.; Ose, T.; Okamoto, N.; Maenaka, K.; Tanaka, T.; Masai, H.; Saito, M.; Shirai, T.; Kohda, D. Structural basis of the 3'-end recognition of a leading strand in stalled replication forks by PriA. *EMBO J.* **2007**, *26*, 2584–2593.
- (35) Lee, M. S.; Marians, K. J. Escherichia coli replication factor Y, a component of the primosome, can act as a DNA helicase. *Proc. Natl. Acad. Sci. U.S.A.* **1987**, *84*, 8345–8349.
- (36) Lasken, R. S.; Kornberg, A. The primosomal protein n' of Escherichia coli is a DNA helicase. *J. Biol. Chem.* **1988**, *263*, 5512–5518.
- (37) Singleton, M. R.; Dillingham, M. S.; Wigley, D. B. Structure and mechanism of helicases and nucleic acid translocases. *Annu. Rev. Biochem.* **2007**, *76*, 23–50.
- (38) Wang, Y.; Sun, Z.; Bianco, P. R.; Lyubchenko, Y. L. Atomic force microscopy-based characterization of the interaction of PriA helicase with stalled DNA replication forks. *J. Biol. Chem.* **2020**, *295*, 6043–6052.
- (39) Tanaka, T.; Taniyama, C.; Arai, K.-I.; Masai, H. ATPase/helicase motif mutants of Escherichia coli PriA protein essential for recombination-dependent DNA replication. *Genes Cells* **2003**, *8*, 251–261.
- (40) Jones, J. M.; Nakai, H. Escherichia coli PriA helicase: fork binding orients the helicase to unwind the lagging strand side of arrested replication forks. Edited by M. Gottesman. *J. Mol. Biol.* **2001**, *312*, 935–947.
- (41) Arai, K.; Arai, N.; Shlomai, J.; Kornberg, A. Replication of duplex DNA of phage phi X174 reconstituted with purified enzymes. *Proc. Natl. Acad. Sci. U.S.A.* **1980**, *77*, 3322–3326.
- (42) Cadman, C. J.; McGlynn, P. PriA helicase and SSB interact physically and functionally. *Nucleic Acids Res.* **2004**, *32*, 6378–6387.
- (43) Yu, C.; Tan, H. Y.; Choi, M.; Stanenas, A. J.; Byrd, A. K.; Raney, K. D.; Cohan, C. S.; Bianco, P. R. SSB binds to the RecG and PriA helicases in vivo in the absence of DNA. *Genes Cells* **2016**, *21*, 163–184.
- (44) Ding, W.; Tan, H. Y.; Zhang, J. X.; Wilczek, L. A.; Hsieh, K. R.; Mulkin, J. A.; Bianco, P. R. The mechanism of single strand binding

protein-RecG binding: Implications for SSB interactome function. *Protein Sci.* **2020**, *29*, 1211–1227.

(45) Manhart, C. M.; McHenry, C. S. The PriA replication restart protein blocks replicase access prior to helicase assembly and directs template specificity through its ATPase activity. *J. Biol. Chem.* **2013**, *288*, 3989–3999.

(46) Marians, K. J. PriA-directed replication fork restart in *Escherichia coli*. *Trends Biochem. Sci.* **2000**, *25*, 185–189.

(47) Marians, K. J. PriA: at the crossroads of DNA replication and recombination. *Prog. Biophys. Mol. Biol.* **1999**, *63*, 39–67.

(48) Marians, K. J. Mechanisms of replication fork restart in *Escherichia coli*. *Philos. Trans. R. Soc. Lond. Ser. B Biol. Sci.* **2004**, *359*, 71–77.

(49) Zavitz, K. H.; Marians, K. J. ATPase-deficient mutants of the *Escherichia coli* DNA replication protein PriA are capable of catalyzing the assembly of active primosomes. *J. Biol. Chem.* **1992**, *267*, 6933–6940.

(50) Bianco, P. R. DNA Helicase-SSB Interactions Critical to the Regression and Restart of Stalled DNA Replication forks in *Escherichia coli*. *Genes* **2020**, *11*, 471.

(51) Delagoutte, E.; Heneman-Masurel, A.; Baldacci, G. Single-stranded DNA binding proteins unwind the newly synthesized double-stranded DNA of model miniforks. *Biochemistry* **2011**, *50*, 932–944.

(52) Liu, X.; Seet, J. X.; Shi, Y.; Bianco, P. R. Rep and UvrD Antagonize One Another at Stalled Replication Forks and This Is Exacerbated by SSB. *ACS Omega* **2019**, *4*, 5180–5196.

(53) Sun, Z.; Tan, H. Y.; Bianco, P. R.; Lyubchenko, Y. L. Remodeling of RecG Helicase at the DNA Replication Fork by SSB Protein. *Sci. Rep.* **2015**, *5*, 9625.

(54) Bhattacharyya, B.; George, N. P.; Thurmes, T. M.; Zhou, R.; Jani, N.; Wessel, S. R.; Sandler, S. J.; Ha, T.; Keck, J. L. Structural mechanisms of PriA-mediated DNA replication restart. *Proc. Natl. Acad. Sci. U.S.A.* **2014**, *111*, 1373–1378.

(55) Sun, Z.; Wang, Y.; Bianco, P. R.; Lyubchenko, Y. L. Dynamics of the PriA Helicase at Stalled DNA Replication Forks. *J. Phys. Chem. B* **2021**, *125*, 4299. in press

(56) Abd Wahab, S.; Choi, M.; Bianco, P. R. Characterization of the ATPase activity of RecG and RuvAB proteins on model fork structures reveals insight into stalled DNA replication fork repair. *J. Biol. Chem.* **2013**, *288*, 26397–26409.

(57) Bianco, P. R. The tale of SSB. *Prog. Biophys. Mol. Biol.* **2017**, *127*, 111–118.

(58) Huang, Y.-H.; Huang, C.-Y. The glycine-rich flexible region in SSB is crucial for PriA stimulation. *RSC Adv.* **2018**, *8*, 35280–35288.

(59) Kozlov, A. G.; Jezewska, M. J.; Bujalowski, W.; Lohman, T. M. Binding Specificity of *Escherichia coli* Single-Stranded DNA Binding Protein for the  $\chi$  Subunit of DNA pol III Holoenzyme and PriA Helicase. *Biochemistry* **2010**, *49*, 3555–3566.

(60) McGlynn, P.; Mahdi, A.; Lloyd, R. Characterisation of the catalytically active form of RecG helicase. *Nucleic Acids Res.* **2000**, *28*, 2324–2332.

(61) McGlynn, P.; Lloyd, R. G. RecG helicase activity at three- and four-strand DNA structures. *Nucleic Acids Res.* **1999**, *27*, 3049–3056.

(62) McGlynn, P.; Lloyd, R. G. Rescue of stalled replication forks by RecG: simultaneous translocation on the leading and lagging strand templates supports an active DNA unwinding model of fork reversal and Holliday junction formation. *Proc. Natl. Acad. Sci. U.S.A.* **2001**, *98*, 8227–8234.

(63) Harmon, F. G.; Kowalczykowski, S. C. Biochemical characterization of the DNA helicase activity of the *Escherichia coli* RecQ helicase. *J. Biol. Chem.* **2001**, *276*, 232–243.

(64) Joo, C.; McKinney, S. A.; Lilley, D. M. J.; Ha, T. Exploring rare conformational species and ionic effects in DNA Holliday junctions using single-molecule spectroscopy. *J. Mol. Biol.* **2004**, *341*, 739–751.

(65) Fogg, J. M.; Kvaratskhelia, M.; White, M. F.; Lilley, D. M. J. Distortion of DNA junctions imposed by the binding of resolving enzymes: a fluorescence study. *J. Mol. Biol.* **2001**, *313*, 751–764.

(66) Kitzing, E. v.; Lilley, D. M.; Diekmann, S. The stereochemistry of a four-way DNA junction: a theoretical study. *Nucleic Acids Res.* **1990**, *18*, 2671–2683.

(67) Every, A. E.; Russu, I. M. Influence of magnesium ions on spontaneous opening of DNA base pairs. *J. Phys. Chem. B* **2008**, *112*, 7689–7695.

(68) Wyatt, H. D. M.; West, S. C. Holliday junction resolvases. *Cold Spring Harbor Perspect. Biol.* **2014**, *6*, a023192.

(69) Gregg, A. V.; McGlynn, P.; Jaktaji, R. P.; Lloyd, R. G. Direct rescue of stalled DNA replication forks via the combined action of PriA and RecG helicase activities. *Mol. Cell* **2002**, *9*, 241–251.

(70) Singleton, M. R.; Scaife, S.; Wigley, D. B. Structural analysis of DNA replication fork reversal by RecG. *Cell* **2001**, *107*, 79–89.

(71) Tanaka, T.; Masai, H. Stabilization of a stalled replication fork by concerted actions of two helicases. *J. Biol. Chem.* **2006**, *281*, 3484–3493.

(72) Wu, H. Y.; Lu, C. H.; Li, H. W. RecA-SSB Interaction Modulates RecA Nucleoprotein Filament Formation on SSB-Wrapped DNA. *Sci. Rep.* **2017**, *7*, 11876.

(73) Zhou, R.; Kozlov, A. G.; Roy, R.; Zhang, J.; Korolev, S.; Lohman, T. M.; Ha, T. SSB functions as a sliding platform that migrates on DNA via reptation. *Cell* **2011**, *146*, 222–232.

(74) Manosas, M.; Perumal, S. K.; Bianco, P. R.; Ritort, F.; Benkovic, S. J.; Croquette, V. RecG and UvsW catalyze robust DNA rewinding critical for stalled DNA replication fork rescue. *Nat. Commun.* **2013**, *4*, 2368.

(75) Tan, H. Y.; Wilczek, L. A.; Pottinger, S.; Manosas, M.; Yu, C.; Nguyenduc, T.; Bianco, P. R. The intrinsically disordered linker of *E. coli* SSB is critical for the release from single-stranded DNA. *Protein Sci.* **2017**, *26*, 700–717.

(76) Schmidt, A.; Kochanowski, K.; Vedelaar, S.; Ahn, E.; Volkmer, B.; Callipo, L.; Knoop, K.; Bauer, M.; Aebersold, R.; Heinemann, M. The quantitative and condition-dependent *Escherichia coli* proteome. *Nat. Biotechnol.* **2016**, *34*, 104–110.

(77) Lewis, J. S.; Jergic, S.; Dixon, N. E. The *E. coli* DNA Replication Fork. *Enzymes* **2016**, *39*, 31–88.

(78) Zhao, T.; Liu, Y.; Wang, Z.; He, R.; Xiang Zhang, J.; Xu, F.; Lei, M.; Deci, M. B.; Nguyen, J.; Bianco, P. R. Super-resolution imaging reveals changes in *Escherichia coli* SSB localization in response to DNA damage. *Genes Cells* **2019**, *24*, 814–826.

(79) Gill, S. C.; von Hippel, P. H. Calculation of protein extinction coefficients from amino acid sequence data. *Anal. Biochem.* **1989**, *182*, 319–326.

(80) Lohman, T. M.; Green, J. M.; Beyer, R. S. Large-scale overproduction and rapid purification of the *Escherichia coli* *ssb* gene product. Expression of the *ssb* gene under  $\lambda$  PL control. *Biochemistry* **1986**, *25*, 21–25.

(81) Liu, J.; Choi, M.; Stanenas, A. G.; Byrd, A. K.; Raney, K. D.; Cohan, C.; Bianco, P. R. Novel, fluorescent, SSB protein chimeras with broad utility. *Protein Sci.* **2011**, *20*, 1005–1020.

(82) Nossal, N. G.; Hinton, D. M.; Hobbs, L. J.; Spacciopoli, P. [43] Purification of bacteriophage T4 DNA replication proteins. *Methods Enzymol.* **1995**, *262*, 560–584.

(83) Bianco, P. R.; Hurley, E. M. The type I restriction endonuclease EcoR124I, couples ATP hydrolysis to bidirectional DNA translocation. *J. Mol. Biol.* **2005**, *352*, 837–859.

(84) Jensen, D. E.; Kelly, R. C.; von Hippel, P. H. DNA "melting" proteins. II. Effects of bacteriophage T4 gene 32-protein binding on the conformation and stability of nucleic acid structures. *J. Biol. Chem.* **1976**, *251*, 7215–7228.

(85) Segel, I. H. *Biochemical calculations*, 2nd ed.; John Wiley and Sons: Hoboken, NJ, 1976.